Near-zero-index wires

La Spada, L & Vegni, L

Original citation:
La Spada, L & Vegni, L 2017, 'Near-zero-index wires' *Optics Express*, vol 25, no. 20, pp. 23699-23708
https://dx.doi.org/10.1364/OE.25.023699

DOI 10.1364/OE.25.023699
ESSN 1094-4087

Publisher: Optical Society of America

Research Article | Vol. 25, No. 20 | 2 Oct 2017 | OPTICS EXPRESS 23699
Optics EXPRESS

Near-zero-index wires

LUIGI LA SPADA[1,*] AND LUCIO VEGNI[2,3]

[1]School of Electronic Engineering and Computer Science, Queen Mary University of London, London E1 4NS, UK
[2]Department of Engineering, University of Roma Tre, Via Vito Volterra 62, Rome 00146, Italy
[3]lucio.vegni@uniroma3.it
*l.laspada@qmul.ac.uk

Abstract: In this work, near-zero-index material boundary properties have been exploited to achieve new electromagnetic functionalities. The extraordinary guiding properties of a cylindrical dielectric rod waveguide surrounded by a thin epsilon-mu-near-zero shell is analyzed and discussed. A closed-form solution for the dispersion equation has been developed, able to model and design such properties at will. Analytical and numerical results will confirm that the use of near-zero cover materials leads to extraordinary properties in terms of field configurations, low attenuation, and bandwidth. The dielectric wire acts as an efficient "waveguide" with great potentials for advance nanocircuit and electronics.

OCIS codes: (160.3918) Metamaterials; (230.7370) Waveguides; (240.6690) Surface waves; (260.2110) Electromagnetic optics; (350.4600) Optical engineering; (060.0060) Fiber optics and optical communications.

References and links

1. L. O. Goldstone and A. A. Oliner, "Leaky wave antennas I: Rectangular waveguides," IRE Trans. Antennas Propag. **7**(4), 307–319 (1959).
2. L. O. Goldstone and A. A. Oliner, "Leaky wave antennas II: Circular waveguides," IRE Trans. Antennas Propag. **9**(3), 280–290 (1961).
3. S. Ramo, J. R. Whinnery, and T. Van Duzer, *Fields and Waves in Communication Electronics*, Second Edition, (John Wiley & Sons, New York, 1984).
4. P. K. Tien, "Light waves in thin films and integrated optics," Appl. Opt. **10**(11), 2395–2413 (1971).
5. N. Marcuvitz, *Waveguide Handbook* (McGraw-Hill, New York, 1951).
6. E. Snitzer, "Cylindrical electric waveguide modes," J. Opt. Soc. Am. **51**(5), 491–498 (1961).
7. R. E. Collin, *Field Theory of Guided Waves* (McGraw-Hill, New York, 1960).
8. L. Bailin and S. Silver, "Exterior electromagnetic boundary value problems for spheres and cones," IRE Trans. Antennas Propag. **4**(1), 5–16 (1956).
9. A. W. Snyder, "Asymptotic expressions for eigenfunctions and eigenvalues of a dielectric or optical waveguide," IEEE Trans. Microw. Theory Tech. **17**(12), 1130–1138 (1969).
10. A. W. Snyder, "Excitation and scattering of modes on a dielectric or optical fiber," IEEE Trans. Microw. Theory Tech. **17**(12), 1138–1144 (1969).
11. B. Liedberg, C. Nylander, and I. Lunstrom, "Surface plasmon resonance for gas detection and biosensing," Sens. Actuators **4**, 299–304 (1983).
12. J. Homola, S. S. Yee, and G. Gauglitz, "Surface plasmon resonance sensors: Review," Sens. Actuat. B **54**(1-2), 3–15 (1999).
13. A. Lahav, M. Auslender, and I. Abdulhalim, "Sensitivity enhancement of guided-wave surface-plasmon resonance sensors," Opt. Lett. **33**(21), 2539–2541 (2008).
14. R. Wang, H. Xia, D. Zhang, J. Chen, L. Zhu, Y. Wang, E. Yang, T. Zang, X. Wen, G. Zou, P. Wang, H. Ming, R. Badugu, and J. R. Lakowicz, "Bloch surface waves confined in one dimension with a single polymeric nanofibre," Nat. Commun. **8**, 14330 (2017).
15. W. Peng, S. Banerji, Y. C. Kim, and K. S. Booksh, "Investigation of dual-channel fiber-optic surface plasmon resonance sensing for biological applications," Opt. Lett. **30**(22), 2988–2990 (2005).
16. C. Caucheteur, T. Guo, F. Liu, B.-O. Guan, and J. Albert, "Ultrasensitive plasmonic sensing in air using optical fibre spectral combs," Nat. Commun. **7**, 13371 (2016).
17. L. Wei, H. Yanyi, X. Yong, K. L. Reginald, and Y. Amnon, "Highly sensitive fiber Bragg grating refractive index sensors," Appl. Phys. Lett. **86**(15), 151122 (2005).
18. M. Loncar, "Molecular sensors: Cavities lead the way," Nat. Photonics **1**(10), 565–567 (2007).
19. N. Engheta and R. W. Ziolkowski, *Metamaterials: Physics and Engineering Explorations* (Wiley, 2006).
20. I. Liberal and N. Engheta, "Near-zero refractive index photonics," Nat. Photonics **11**(3), 149–158 (2017).
21. I. V. Lindell and A. H. Sihvola, "Electromagnetic boundary and its realization with anisotropic metamaterial," Phys. Rev. E Stat. Nonlin. Soft Matter Phys. **79**(2 Pt 2), 026604 (2009).

#300539 https://doi.org/10.1364/OE.25.023699
Journal © 2017 Received 21 Jun 2017; revised 26 Jul 2017; accepted 5 Aug 2017; published 18 Sep 2017

Optics EXPRESS

22. I. V. Lindell and A.H. Sihvola, "Realization of the PEMC boundary," in IEEE Transactions on Antennas and Propagation **53**(9), 3012–3018 (2005).
23. N. Engheta, A. Salandrino, and A. Alù, "Circuit elements at optical frequencies: nanoinductors, nanocapacitors, and nanoresistors," Phys. Rev. Lett. **95**(9), 095504 (2005).
24. N. Engheta, "Circuits with light at nanoscales: optical nanocircuits inspired by metamaterials," Science **317**(5845), 1698–1702 (2007).
25. A. Alù and N. Engheta, "All optical metamaterial circuit board at the nanoscale," Phys. Rev. Lett. **103**(14), 143902 (2009).
26. B. Edwards and N. Engheta, "Experimental verification of displacement-current conduits in metamaterials-inspired optical circuitry," Phys. Rev. Lett. **108**(19), 193902 (2012).
27. Y. Li, I. Liberal, C. Della Giovampaola, and N. Engheta, "Waveguide metatronics: Lumped circuitry based on structural dispersion," Sci. Adv. **2**(6), e1501790 (2016).
28. R. Liu, C. M. Roberts, Y. Zhong, V. A. Podolskiy, and D. Wasserman, "Epsilon-near-zero photonics wires," ACS Photonics **3**(6), 1045–1052 (2016).
29. V. Rumsey, "Some new forms of Huygens' principle," IRE Trans. Antennas Propag. **7**(5), 103–116 (1959).
30. A. D. Yaghjian and S. Maci, "Alternative derivation of electromagnetic cloaks and concentrators," New J. Phys. **10**(11), 115022 (2008).
31. C. A. Balanis, *Antenna Theory: Analysis and Design*, 3rd Edition (John Wiley & Sons, 2005).
32. C. H. Chandler, "An investigation of dielectric rod as waveguide," J. Appl. Phys. **20**(12), 1188–1192 (1949).
33. D. Marcuse, *Theory of Dielectric Optical Waveguide, Academic* (Elsevier, 1974).
34. I. V. Lindell, "Condition for the general ideal boundary," Microw. Opt. Technol. Lett. **26**(1), 61–64 (2000).
35. A. Alù and N. Engheta, "Optical 'shorting wires'," Opt. Express **15**(21), 13773–13782 (2007).
36. I. Liberal, A. M. Mahmoud, Y. Li, B. Edwards, and N. Engheta, "Photonic doping of epsilon-near-zero media," Science **355**(6329), 1058–1062 (2017).
37. A. Alù, F. Bilotti, N. Engheta, and L. Vegni, "Theory and simulations of a conformal omni-directional subwavelength metamaterial leaky-wave antenna," IEEE Trans. Antenn. Propag. **55**(6), 1698–1708 (2007).
38. Y. Jin and S. He, "Enhancing and suppressing radiation with some permeability-near-zero structures," Opt. Express **18**(16), 16587–16593 (2010).
39. J. W. Duncan and R. H. DuHamel, "A technique for controlling the radiation from dielectric rod waveguides," IRE Trans. Antennas Propag. **5**(3), 284–289 (1957).
40. A. M. Mahmoud, I. Liberal, and N. Engheta, "Dipole-dipole interactions mediated by epsilon-and-mu-near-zero waveguide supercoupling," Opt. Mater. Express **7**(2), 415–424 (2017).
41. A. M. Mahmoud and N. Engheta, "Wave-matter interactions in epsilon-and-mu-near-zero structures," Nat. Commun. **5**, 5638 (2014).
42. V. Torres, V. Pacheco-Peña, P. Rodríguez-Ulibarri, M. Navarro-Cía, M. Beruete, M. Sorolla, and N. Engheta, "Terahertz epsilon-near-zero graded-index lens," Opt. Express **21**(7), 9156–9166 (2013).
43. L. La Spada and L. Vegni, "Metamaterial-based wideband electromagnetic wave absorber," Opt. Express **24**(6), 5763–5772 (2016).
44. R. Maas, J. Parsons, N. Engheta, and A. Polman, "Experimental realization of an epsilon-near-zero metamaterial at visible wavelengths," Nat. Photonics **7**(11), 907–912 (2013).
45. CST STUDIO SUITETM, (CST of Europe Inc. 2016), www.cst.com.
46. D. Kajfez and P. Guillon, *Dielectric Resonators* (Artech House, Inc., 1986).
47. R. F. Harrington, *Time-Harmonic Electromagnetic Fields* (McGraw-Hill, 1961).

1. Introduction

The possibility to control electromagnetic waves, and their propagating properties from microwave to optics, is of great interest. Waveguide structures are crucial in several applications fields such as telecommunications [1,2], detection [3], absorption and energy harvesting [4]. Several examples of guiding structures are present in literature such as: rectangular [5], circular [6] and radial [7] waveguides, spherical transmission lines [8], and fibers cables [9,10]. Waveguide structures have been used recently in optics for bio-chemical sensing devices [11], improved by the development of surface plasmon resonance (SPR) phenomenon [12]. More specifically, thanks to the recent fabrication advancements, different structures in SPR sensing systems have been proposed such as: dielectric waveguides [13, 14], fiber sensors schemes [15, 16], gratings [17], and plasmonic cavities [18]

Despite all such technology variety, several problems are still present: dispersive behavior due to the materials used, fixed and narrow operational bandwidth dependent on the structure geometry and dimensions, losses (radiation and attenuation) caused by the presence of abrupt changes in the propagation path such as tips, sharp corners, and discontinuities. Near-Zero Index (NZI) materials [19] can represent a valid solution to such problems. Thanks to their unusual constitutive parameters values (electric permittivity and/or magnetic permeability

Optics EXPRESS

approaching to zero) they exhibit exotic wave-matter interaction phenomena [20]. Among them, here we focus our attention on two distinctive properties: the electric D = εE and/or magnetic B = μH flux density vanishing in Epsilon-Near-Zero (ENZ) and Mu-Near-Zero (MNZ) media, respectively [21]; and the possibility that both D and B vectors simultaneously vanish within an Epsilon-Mu-Near-Zero (EMNZ) medium, the so-called Double-Bounded (DB) structure [22]. In the past, such phenomena have been studied separately, and different applications were developed.

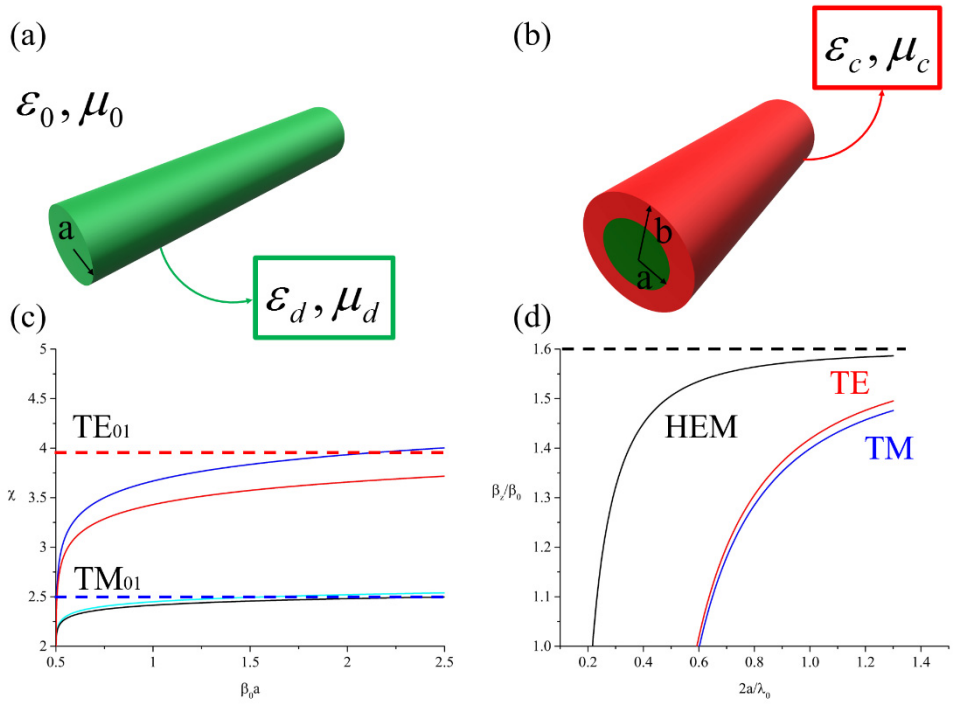

Fig. 1. (a) Dielectric rod (ε_d = 38, $\mu_d = \mu_0$); (b) Folded-Dielectric Rod (ε_c = 2.56, $\mu_c = \mu_0$); (c) Dispersion curves for: HEM (black), TM (blue), TE (red), TM for ENZ cover (cyan), TE_{01} (red, dot) and TM_{01} (blue dot) for EMNZ cover; (d) Ratio of β_z/β_0, for first three surface-wave modes on the dielectric rod.

Due to the vanishing of electric D (magnetic B) flux, it is possible to guide the displacement electric (magnetic) current along such structures. The phenomenon is like what happens in traditional conducting wires where, metal guides the flow of the conduction current. Such an idea has been exploited for the development of optical metatronics components [23, 24] or D-dot wires [25], and recently experimentally validated in the microwave [26, 27], and in the mid-infrared [28] frequency regime. For the DB boundary condition property, at the beginning the interest was mainly theoretical, aiming to develop new electromagnetic equivalence principles [29], and initial practical applications were developed due to the unusual scattering properties [30].

Here, by combining both phenomena we will develop electromagnetic structures able to achieve new and exotic propagation properties. First, we will present a generalized modeling approach to describe its electromagnetic and geometric characteristics: it provides a detailed description of the structure field configurations (modes). Then, by applying the related boundary conditions, the design step will be reported: such step is crucial, giving us the possibility to develop structures accordingly to a specific required application. Finally, to validate modeling and design procedures a NZI dielectric wire realization is studied: it will

Optics EXPRESS

show how such a double bounded structure is able to replace traditional metallic wires by mimicking their behavior, and at the same time overcome their issues such as attenuation, losses, and dispersive behavior.

2. Near-zero-index waveguides modeling

For different electromagnetic boundary-value problems, there are usually many modes that are solutions satisfying Maxwell's equations and the boundary conditions: Transverse Electric (TE) and Transverse Magnetic (TM) modes possess the electric (magnetic) field component perpendicular to the propagation direction z. Any other modes can be considered as superimposition of both: such as Transverse ElectroMagnetic (TEM) with the electric and magnetic field present on the transverse plane; or Hybrid ElectroMagnetic (HEM) modes, combinations of both TE and TM. Here we will focus on cylindrical-symmetry waveguides due to their popularity for being easy to realize and possessing low attenuation of the TE0n modes. Similar results and conclusions can be achieved for any other waveguide shape and geometry, in any coordinate systems we can envision. Let's start from a classical rod (core) with radius a and constitutive parameters ε_d and μ_d, Fig. 1(a), folded by a cover of radius b, with permittivity and permeability as ε_c and μ_c, Fig. 1(b). The surrounding region is assumed to be free space with permittivity ε_0 and permeability μ_0. To maintain some simplicity in the mathematics, we will consider only solution for the electric **E** and magnetic **H** fields in a source-free and lossless media. The procedure is valid also for more complicated, real-life structures (considering losses) from low frequencies (RF/microwave) to higher frequencies (infrared/optics).

Independently from the considered mode, the wave vector equation should be solved for the vector potential **A** (magnetic)/**F** (electric) for TM/TE modes along the z propagation direction (P_z) and expanded in cylindrical coordinates (ρ, ϕ, z). By separation of variables the solution has the form:

$$P_z = \left[af_1(\rho) + bf_2(\rho)\right] \cdot \left[cg_1(\varphi) + dg_2(\varphi)\right] \cdot \left[eh_1(z) + fh_2(z)\right] \quad (1)$$

Functions f(ρ), g(ϕ), and h(z) can take different expressions, depending on the configuration of the problem (geometry/shape) and the region (core/cover/air). The transverse functions represent standing waves, while the longitudinal ones are travelling waves.

A dielectric rod can support only a finite number of unattenuated modes, with their fields localized in the center (ρ ≤ a). Within the rod along the three directions we can have: standing waves in the radial ρ direction ($f_1(\rho) = J_m(\beta_d\rho)$ Bessel functions of m-th order and first kind, $f_2(\rho) = 0$); periodic waves in the azimuthal φ direction ($g_1(\phi) = \cos(m\phi)$ and $g_2(\phi) = \sin(m\phi)$), and traveling waves (exponential functions) in the z direction ($h_1(z) = e^{-j\beta z}$ and $h_2(z) = 0$).

A similar field structure can exist in the cover (a ≤ ρ ≤ b), with only the difference that both Bessel functions of first and second kind represent the standing waves ($f_1(\rho) = J_m(\beta d\rho)$ and $f_2(\rho) = Y_m(\beta_d\rho)$) in the radial direction.

The fields outside the rod (ρ ≥ b) can be outward radial travelling waves (Hankel functions of the second kind $f_1(\rho) = H_m^{(2)}(\beta_d\rho)$ and $f_2(\rho) = 0$) or of evanescent type, surface wave modes (modified Bessel functions of the second kind $f_1(\rho) = K_m(\alpha\rho)$).

Once the potential vector A_z (F_z) is found, the next step is to find the corresponding electric **E** and magnetic **H** field components. By using [31], the related expressions for hybrid modes can be founded:

Optics EXPRESS

$$\begin{cases} E_\rho = -\left(\frac{1}{\varepsilon}\frac{1}{\rho}\partial_\varphi P^{TE} + j\frac{1}{\omega\mu\varepsilon}\partial_\rho\partial_\varphi P^{TM}\right) \\ E_\varphi = \left(\frac{1}{\varepsilon}\partial_\rho P^{TE} - j\frac{1}{\omega\mu\varepsilon}\frac{1}{\rho}\partial_\varphi\partial_z P^{TM}\right) \\ E_z = \left(j\frac{1}{\omega\mu\varepsilon}\partial_z^2 + \beta\right)P^{TM} \end{cases} \quad \begin{cases} H_\rho = -j\frac{1}{\omega\mu\varepsilon}\partial_\rho\partial_z P^{TE} + \frac{1}{\mu}\frac{1}{\rho}\partial_\varphi P^{TM} \\ H_\varphi = -\left(j\frac{1}{\omega\mu\varepsilon}\frac{1}{\rho}\partial_\varphi\partial_z P^{TE} + \frac{1}{\mu}\partial_\rho P^{TM}\right) \\ H_z = \left(-j\frac{1}{\omega\mu\varepsilon}\partial_z^2 + \beta\right)P^{TE} \end{cases} \quad (2)$$

Expressions for classical TE/TM modes can be easily found by selecting the proper scalar wave potential P_z. Pure TE/TM modes exist only when the field configurations are symmetrical and independent of φ [32]; instead field configurations that are combinations of TE and TM modes can be nonsymmetrical and possess angular φ variations, usually referred to as hybrid HEM modes [33].

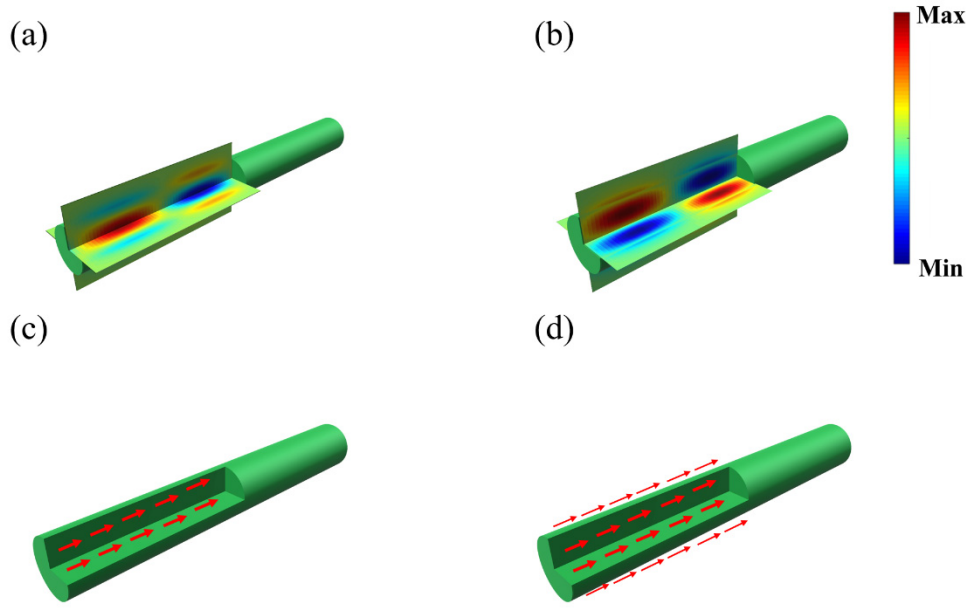

Fig. 2. Field Configurations for Dielectric Rod for (a) Electric Field (HEM, TM); (b) Electric Field (TM). Poynting vector for (c) HEM and (d) TE and TM. Values used: a = λ/20, l = 2λ, ε_d = 38, $\mu_d = \mu_0$.

3. Near-zero-index waveguides design

It is evident from all the possible core-shell combinations that we can have three different structures with their own properties: unbounded (folded) rod, by using the traditional Double PoSitive materials (DPS) for both core and cover; single bounded: DPS core and electric (magnetic)-near-zero material as cover (ENZ or MNZ); and double bounded: DPS core and double-near-zero material as cover (EMNZ). The field configurations (modes) that can be supported inside such structures depend on their boundary characteristics:

- Tangential electric/magnetic conservation at the interface [34]: i.e. dielectric core – dielectric cover (unbounded structures).

Optics EXPRESS

- Tangential magnetic field vanishing [35, 36]: perfect magnetic conductor PMC, obtained at boundaries by using materials whose permittivity approaches to zero, $\varepsilon_r \to 0$ (magnetic single bounded structures).
- Tangential electric field vanishing [37, 38]: perfect electric conductor PEC, achieved by their magnetic equivalent, $\mu_r \to 0$ (electric single bounded structures).
- Tangential and normal electric/magnetic component vanishing [39, 40]: the generalized PEMC boundary conditions, obtained when both epsilon and mu approach simultaneously zero (double bounded structures).

The scattering coefficients are not independent of each other and their relation (dispersion equation) can be found by applying the appropriate boundary conditions, for the following structures: dielectric rod – dielectric cover, dielectric rod – ENZ cover and dielectric rod – EMNZ cover:

$$\begin{cases} \mathrm{n}\times\mathrm{E}=0 \\ \mathrm{n}\bullet\mathrm{D}=0 \end{cases} \Rightarrow \det \begin{vmatrix} \frac{\varepsilon_d}{\varepsilon_c}E_\rho^d & -E_\rho^c\left(f_1(\rho)\right) & -E_\rho^c\left(f_2(\rho)\right) & 0 \\ E_\varphi^d & -E_\varphi^c\left(f_1(\rho)\right) & -E_\varphi^c\left(f_2(\rho)\right) & 0 \\ 0 & E_\rho^c\left(f_1(\rho)\right) & E_\rho^c\left(f_2(\rho)\right) & -\frac{\varepsilon_0}{\varepsilon_c}E_\rho^0 \\ 0 & E_\varphi^c\left(f_1(\rho)\right) & E_\varphi^c\left(f_2(\rho)\right) & -E_\varphi^0 \end{vmatrix} \tag{3}$$

$$\overset{TM}{\Rightarrow} \frac{J_0'(\chi_{0n})}{\chi_{0n}} + \frac{K_0'(\xi_{0n})J_0(\chi_{0n})}{\varepsilon_d\xi_{0n}K_0(\xi_{0n})} = -\frac{J_1(\chi_{0n})}{\chi_{0n}} - \frac{K_1(\xi_{0n})J_0(\chi_{0n})}{\varepsilon_d\xi_{0n}K_0(\xi_{0n})}$$

$$\begin{cases} \mathrm{n}\times\mathrm{H}=0 \\ \mathrm{n}\bullet\mathrm{D}=0 \end{cases} \Rightarrow \det \begin{vmatrix} \frac{\varepsilon_d}{\varepsilon_c}E_\rho^d & -E_\rho^c\left(f_1(\rho)\right) & -E_\rho^c\left(f_2(\rho)\right) & 0 \\ H_{\varphi,z}^d & -H_{\varphi,z}^c\left(f_1(\rho)\right) & -H_{\varphi,z}^c\left(f_2(\rho)\right) & 0 \\ 0 & E_\rho^c\left(f_1(\rho)\right) & E_\rho^c\left(f_2(\rho)\right) & -\frac{\varepsilon_0}{\varepsilon_c}E_\rho^0 \\ 0 & H_{\varphi,z}^c\left(f_1(\rho)\right) & H_{\varphi,z}^c\left(f_2(\rho)\right) & -H_{\varphi,z}^0 \end{vmatrix} \tag{4}$$

$$\overset{TM}{\Rightarrow} \det \begin{vmatrix} J_1(\beta_0 a) & -\frac{\varepsilon_c}{\varepsilon_d}J_1(\beta_d a) & -\frac{\varepsilon_c}{\varepsilon_d}Y_1(\beta_d a) & 0 \\ \beta_d J_0(\beta_0 a) & -\beta_c J_0(\beta_c a) & -\beta_c Y_0(\beta_c a) & 0 \\ 0 & -\frac{\varepsilon_c}{\varepsilon_0}J_1(\beta_d b) & -\frac{\varepsilon_c}{\varepsilon_0}Y_1(\beta_d b) & H_1^{(2)}(\beta_0 b) \\ 0 & -\beta_c J_0(\beta_c b) & -\beta_c Y_0(\beta_c b) & H_0^{(2)}(\beta_0 b) \end{vmatrix} = 0$$

$$\begin{cases} \mathrm{n}\times\left(\mathrm{H}+M\mathrm{E}\right)=0 \\ \mathrm{n}\bullet\left(\mathrm{D}-M\mathrm{B}\right)=0 \end{cases} \Rightarrow \det \begin{vmatrix} E_\rho & -M\frac{\mu_d}{\varepsilon_d}H_\rho \\ H_\varphi & ME_\varphi \end{vmatrix} \overset{TM}{\Rightarrow} M\left(1-\frac{\mu_d}{\varepsilon_d}\right)J_0(\chi)J_1(\chi)=0 \tag{5}$$

where $\chi=\beta_d\rho, \xi=\sqrt{(\beta_0 a)^2(\varepsilon_d\mu_d-1)-\chi^2}$, *d*, *c*, *0* and *M* denote dielectric, cover, air, and scalar admittance parameter, respectively. Expressions analogous to Eqs. (3), (4) and (5), may be written for the TE case using duality and by substituting the ratio with unity, and vice versa. It is simple to see how Eqs. (3) and (4) are the generalization of [37] and [35],

Optics EXPRESS

respectively. Equations (3), (4) and (5) can be used to determine the modes supported by the structure to design it accordingly to specific required applications.

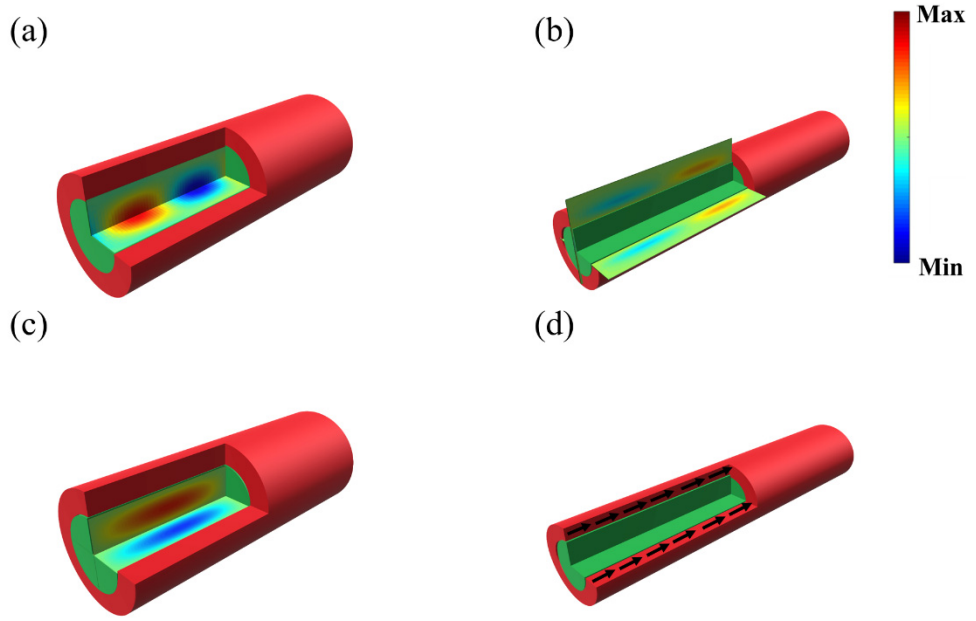

Fig. 3. Field Configurations for Dielectric Rod -ENZ cover for (a) Electric Field (HEM); (b) Electric Field (TM); (c) Magnetic Field (TE). (d) Poynting vector. Values used: a = λ/20, l = 2λ, $\varepsilon_d = 38$, $\mu_d = \mu_0$, $\varepsilon_c = 0.01$, $\mu_c = 1$.

4. Results and discussion

The most salient feature exhibited by near-zero metamaterials is that, unlike naturally occurring materials, they can achieve their electromagnetic properties from their geometry and the frequency range they are considered, rather than their chemistry or composition. To a rough approximation, the wavelength associated with the metamaterial resonant frequency is proportional to the dimension *l* of the electric/magnetic inclusions used. Therefore, in theory, metamaterials may be fashioned to operate over all frequencies by simple scaling of *l*. Indeed, examples in microwave [41], terahertz [42], infrared [43], and optical [44] have been demonstrated.

Equation (5) leads to important physical insights and properties for the EMNZ structure. In the following by comparing such structures, we will highlight what are the crucial advantages achieved by using EMNZ materials, in terms of field amplitude and phase, power flow, losses/attenuation, and bandwidth. The comparison is done first analytically, by using the derived closed-form formulas (3), (4) and (5), and then numerically by using full-wave simulation software [45]. Results are shown in Fig. 2, Fig. 3 and Fig. 4 for the dielectric core – dielectric cover, dielectric core – ENZ cover and dielectric core – EMNZ cover, respectively. The results are shown for the HEM mode (first row), TE mode (second row) and TM mode (third row), in terms of electric (left column), magnetic field (central column), and power flow (right column).

Optics EXPRESS

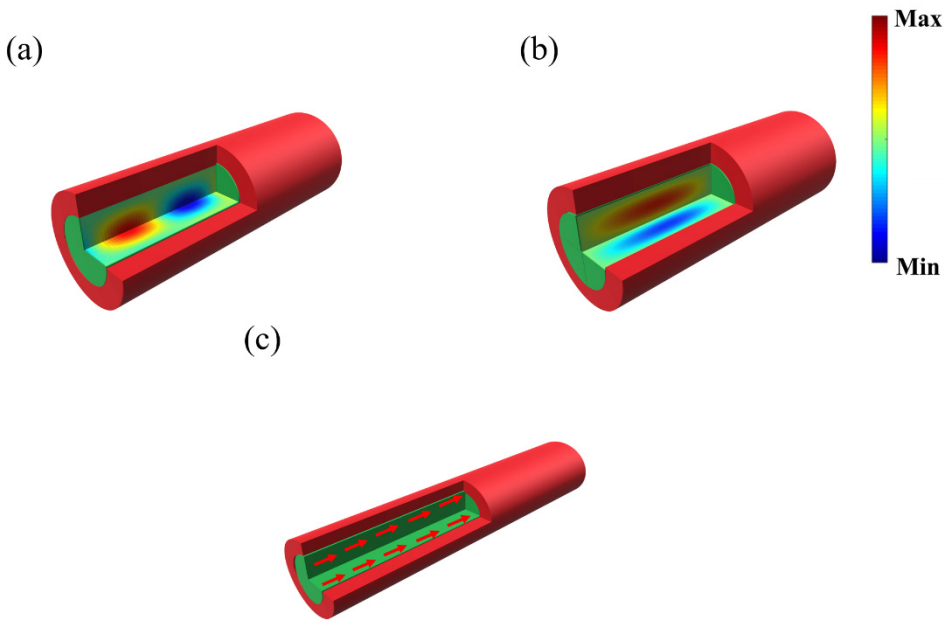

Fig. 4. Field Configurations for Dielectric Rod -EMNZ cover for (a) Electric Field (HEM/TM); (b) Electric Field (TE); (c) Poynting vector. Values used: $a = \lambda/20$, $l = 2\lambda$, $\varepsilon_d = 10$, $\mu_d = \mu_0$, $\varepsilon_c = 0.01$, $\mu_c = 0.01$.

4.1 Field configurations: TE, TM and HEM modes

In a traditional dielectric rod for a given mode the eigenvalues are non-constant and vary as a function of the electrical radius, a/λ [46]. For a traditional (folded) dielectric rod the boundary conditions are highly different from single or double boundary conditions. Both electric and magnetic tangential (normal) components are preserved at the interface, so the dielectric rod admits the existence of non-zero fields, in the cover and outside of it, Figs. 2(a) and 2(b).

In terms of waves typology, let's refer to Fig. 1(c) and 1(d). We can make the following distinction:

- Radiated waves: For values of $\beta^d_\rho a$ greater than χ, the values of $\alpha_{0\rho} a$ become imaginary and according to Eq. (3) and Fig. 1(c), the modified Bessel function of the second kind is reduced to a Hankel function of the second kind that represents unattenuated outwardly traveling waves. In this case, the dielectric rod is acting as a cylindrical antenna because of energy loss from its side.
- Guided waves: The allowable modes in a dielectric rod waveguide are determined by finding the values of χ, that are solutions to the transcendental Eq. (3). It should be noted that for a given mode the values of χ are non-constant and vary as a function of the electrical radius of the rod, Fig. 1(b).
- Surface waves: According to Eq. (3), if the values of χ exceed $\beta_0 a\sqrt{\varepsilon_r}$, then $\beta_z a$ becomes imaginary and the waves in the dielectric rod become decaying (evanescent) along the axis (z direction) of the rod (Fig. 1(d)): for small radii, the fields outside the rod extend to large distances and are said to be loosely bound to the surface; for the larger dielectric constant material, the fields outside the dielectric waveguide are

Optics EXPRESS

more tightly bound to the surface since larger values of β_z translate to larger values of the attenuation coefficient $\alpha_{0\rho}$, Fig. 1(d).

When an ENZ material is used as cover, only the PMC boundary condition should be considered. In other words, the related tangential electric field component is affected by the boundary, leaving the others unaltered. The tangential components vanish because the electric flux density is zero in the ENZ material, Figs. 3(a)-3(c). The ENZ waveguide acts as conducting magnetic wall for TM modes (Fig. 1(c)), whose eigenvalues are constant for the given mode.

When EMNZ materials are implemented as cover, at the interface the shell acts as a very efficient PEMC boundary condition. Both boundary conditions (PMC and PEC) take place, and the admittance M simultaneously affects electric and magnetic field components. Due to the tangential ($\mathbf{H} + M\mathbf{E}$) and normal ($\mathbf{D} - M\mathbf{B}$) components vanishing inside the cover, also the electric ($\mathbf{E}$, $\mathbf{D}$) and magnetic ($\mathbf{H}$, $\mathbf{B}$) fields outside of the structure are zero, Fig. 4(a) and 4(b): all the modes are confined in the structure, having the electric and magnetic fields maximum in the *core*, approaching to zero in the *cover*, no evanescent (surface waves) and/or radiating (fundamental hybrid HEM_{11}) electromagnetic fields are present outside, in contrast with un-bounded and single-bounded structures, Fig. 1(c) and 1(d).

In traditional single boundary structures, such as PMC (ENZ-cover), the cut-off frequencies of the modes TE_{0n} and TM_{1n} are identical (degenerate modes). This is because in the related dispersion equation, the Bessel functions are independent from each other, and the zeroes of the derivative of the Bessel function J_0 are identical to the zeroes of the Bessel function J_1.

On the contrary, for EMNZ-cover guiding structures, their cut-off frequency will depend on the product of both Bessel function $J_m(\beta_d\rho)$ and the derivative $J'_m(\beta_d\rho)$. Differently from single bounded structures, in a PEMC structure the radial functions are not independent anymore, but strictly related each other. Therefore, when the zeros of the J_m Bessel function enable a mode, at the same time they deactivate its derivative J'_m, and vice versa. This give us the possibility to design a structure with non-degenerating propagating modes.

4.2 Poynting vector and energy distribution

In the folded dielectric road configuration, the presence of non-zero electric and magnetic fields leads to the presence of both non-zero tangential and normal Poynting vector: by using Eq. (3) we can separate the modes at the interface cover- air in two main groups: the decaying field waves, called *surface waves* (due to non-zero tangential Poynting vector) and the unattenuated outwardly traveling *radiated waves* (due to non-zero normal Poynting vector), as shown in Fig. 2(c) and 2(d).

When single bounded materials are implemented as covers (ENZ), at the core-shell interface the electric field is longitudinal, whereas in the cover region the field is transversally directed. The main consequence of such behavior is that the *normal* component of the Poynting vector is zero. There is no radiated energy along the radial direction into the air space surrounding the waveguide. On the other hand, the presence of the fields at the interface and in the shell medium and their being orthogonal, leads to a non-zero *tangential* component of the Poynting vector. The Poynting vector is present in the cover shell and it flows inside of it along the propagation direction z, as reported in Fig. 3(d).

In the case of an EMNZ covered waveguide, due to the PEMC boundary conditions no fields exist inside the cover. Both the normal and tangential Poynting vector components are zero. The vanishing of the normal component of the Poynting vector prevents the dielectric rod to irradiate in the free space along the radial component. Most importantly, if also the longitudinal component of the Poynting vector is zero, the cover rejects electromagnetic field longitudinal propagation, and acts as a “perfect” boundary for electromagnetic waves: all the

Optics EXPRESS

fields are localized in the dielectric *core* as well as the Poynting vector, whose component is purely longitudinal and the related power flows along the *z* propagation direction, Fig. 4(c).

The independence of the electric and magnetic fields in un-bounded and single-bounded structures lead to important consequences in terms of energy. If all modes can exist and be excited, the waveguide is in a multimode operation. This can represent a detrimental factor due to the fact the energy will be unfairly distributed along all the modes in the entire system [47]: different modes (non/dominant) can exist at the same time in the structure. All such undesired modes cause distortion and attenuation to the signal.

In double-bounded structures the possibility to isolate the single modes, Eq. (5), lead to the fact that the modes are enable once at a time. The possibility to compartmentalize the modes is crucial. First, because the total power is distributed equally among all the existing modes; secondly and most importantly the related energy is dedicated exclusively to only that mode. The order in which the different modes enter a waveguide still depends upon their cut-off frequency, but they are more repartitioned, compared to the single-bounded cases, or even to a classical dielectric rod. In other words, the EMNZ cover acts as a filter for the components of the undesired modes perpendicular to the propagation direction (which will be damped) and let go through the parallel components of the desired mode (that will remain unaffected).

5. Conclusions

In this paper, a near-zero-index dielectric waveguide is modelled and designed. A generalized analytical approach has been developed to model and design the structure propagation characteristics at will for specific and required applications. An analytical and numerical comparison among the traditional (folded) dielectric rod and the near-zero structures considered, single-bounded (ENZ) and double-bounded (EMNZ), permitted to explore the extraordinary properties of the structure in much physical details and insights. The modelling and design approach simplifies the future device manufacturing process: high permittivity core values are no longer needed to mimic the classical metallic wire behavior. It has been shown that ENZ and EMNZ waveguide are able to overcome the main issues of traditional metallic ones such as: mode degeneration, attenuation/losses, and energy dispersion.